PHYSICAL REVIEW B VOLUME 6, NUMBER 12 15 DECEMBER 1972

Scattering of Low-Energy Electrons from Rare-Gas Crystals Grown on the (100) Face of Nb. I. Electron Diffraction and Desorption*

H. H. Farrell and Myron Strongin
Brookhaven National Laboratory, Upton, New York 11973

and

J. M. Dickey
Queens College of the City University of New York, Flushing, New York 11367
(Received 26 July 1972)

Using low-energy-electron diffraction, we have studied the morphology of thin crystals of the inert gases, neon, argon, krypton, and xenon, which were grown epitaxially on a single-crystal niobium substrate. Neon, argon, and krypton showed marked desorption in the presence of the electron beam even under conditions where it was possible to maintain these crystals indefinitely in the absence of the electron beam. Possible desorption mechanisms are discussed.

I. INTRODUCTION

Using low-energy-electron diffraction (LEED) and a retarding-grid energy analyzer we have studied the morphology, intensity vs energy characteristics, electron-energy-loss spectra, and low-energy Auger spectra of thin crystals of the inert gases neon, argon, krypton, and xenon. In this work we discuss the LEED studies, experimental arrangements, and some measurements of desorption from the surface. In the following paper[1] we discuss the energy-loss spectra. The crystals were between 20- and 100-Å thick and were grown by condensing the gases, typically at pressures of 1×10^{-6} Torr for 1 min, on carefully cleaned single-crystal niobium (100) substrates at temperatures near 7 °K. As previously reported for argon,[2] the three lighter gases showed marked desorption in the presence of the electron beam even under conditions where it was possible to maintain these crystals indefinitely in the absence of the electron beam. The xenon crystals that were investigated appeared to be stable at least over the time span of the experiment, i.e., 2–4 h.

II. APPARATUS

The apparatus we have used in these studies is described in a separate paper.[3] We briefly discuss some of the design features by reference to Fig. 1. Ohmic heating is accomplished by passing current through the sample. This presents a nontrivial design problem since the leads must be capable of supplying currents of up to 50 A to the sample, and then the heat leak must be small at cryogenic temperatures. This was solved by stainless-steel links in the electrical leads (*D*) which isolate the apparatus at liquid-helium temperatures from heat leaks coming down the heavy lead wires from nitrogen temperature and room temperature. It is seen that the sample current flows from (*D*) to plate (*B*) and finally through the sample to plug (*A*). Good cooling is provided by plug (*A*), which projects into the liquid-helium Dewar and is surrounded by liquid helium. Part (*B*) is electrically isolated from ground, but is in moderate thermal contact with the 4.2 °K plug (*A*) through a thin mica cheet (*C*). Hence at cryogenic temperatures part (*B*) is cooled through the mica to about 5 °K, as measured by a carbon thermometer (*J*) on (*B*). During the heating period liquid nitrogen was added to the helium Dewar. The sample could be heated to about 1900 °C and (*B*) only reached a temperature between room and liquid-nitrogen temperature because of the good contact with the plug (*A*), which projected into the liquid nitrogen. To vary the sample temperature at low temperatures, heat was applied to the heater (*H*) on (*B*). The LEED apparatus is a standard Varian 360 system in which the diffraction pattern of the backscattered electrons is displayed on a fluorescent screen. The screen and attendant grids may be used as an energy analyzer by biasing the grids and using the screen as a collector.

III. MORPHOLOGY

In an earlier work, we had observed that argon crystallizes in register on a Nb (100) substrate with pseudo-12-fold symmetry.[2] This was attributed to the growth of domains on basal hexagonal monolayers of argon with two different orientations on the niobium substrate, viz., those with the argon atoms aligned along the niobium (10) direction and those aligned along the (01) direction. An hcp crystal would have true sixfold symmetry in the (0001) face, while an fcc crystal has only threefold symmetry for the (111) face. As there are

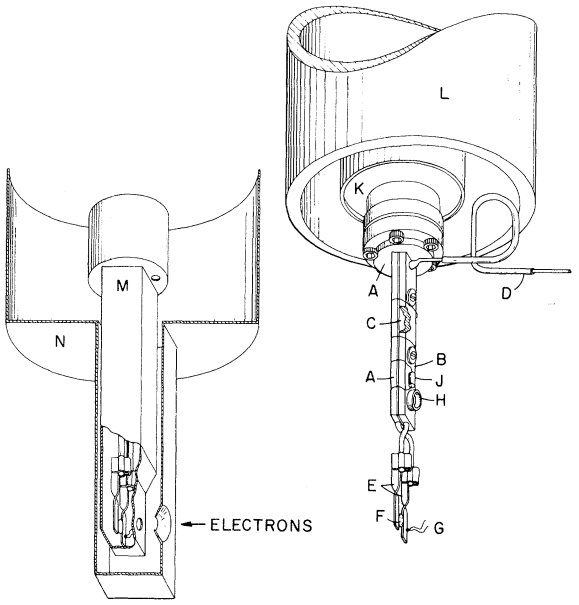

FIG. 1. Sample assembly. *A*, copper plug which extends into helium bath for thermal contact and forms the vacuum seal to the miniflange at the base of the helium Dewar (this block also grounds the sample and provides the return path for the heating current). *B*, copper block attached to hot lead *D* to sample, and is insulated from *A* by the mica *C*. *D*, hot lead to sample with piece of stainless tubing to isolate sample assembly from liquid-nitrogen temperatures. *E*, Nb strip for crystal holder. *F*, Nb crystal. *G*, hot junction of Au–Fe/chromel-*P* thermocouple; the cold junction of the thermocouple is on block *A*. *H*, heater. *J*, carbon thermometer. *K*, helium Dewar. *L*, nitrogen Dewar. *M*, copper shield which fits on bottom of the helium Dewar; the aperture size for electron beam is about 4 mm. *N*, copper shield which fits on bottom of the nitrogen Dewar; the aperture size for electron beam is about 4.8 mm.

two ways to construct an fcc crystal from a basal hexagonal monolayer, both modifications could give pseudo-12-fold symmetry when grown on hexagonal monolayers aligned in the two directions previously described. In the earlier work, it was not possible to distinguish between these two structures.[4–7] However, in the present work it is possible to assign the fcc structure on the basis of intensity data to be discussed below.

The fortuitous match between the niobium lattice parameter 3.29 Å, and the corresponding distance between the close-packed rows in the (111) argon plane 3.32 Å, was taken as the rationale for the violation of the conservation of rotational symmetry usually found in epitaxial growth. When krypton was crystallized on a Nb (100) substrate, the same diffraction pattern was obtained as for argon. This was not surprising as the lattice parameter for krypton is only about 3% larger than that of argon: 5.59 vs 5.43 Å. Neon, however, represents a

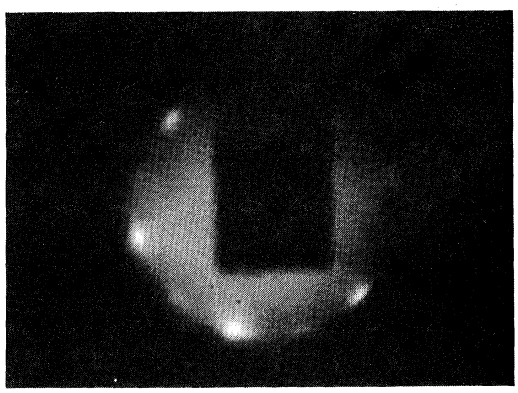

FIG. 2. LEED pattern from the (111) face of neon adsorbed on Nb(100). Dark rectangle in foreground is a cryogenic shield surrounding the sample. Note trace of pseudo-12-fold symmetry.

rather different case, since its lattice parameter 4.52 Å is considerably smaller. Thus, it was somewhat surprising when diffraction patterns were observed for neon condensed on a Nb (100) substrate that were similar to those for argon and krypton (Figs. 2–4). This may be taken as an indication of the relative stability of the (111) face of the face-centered-cubic inert-gas crystals despite the sacrifice in free energy necessary to overcome the ~18% lattice mismatch between the neon (111) face and the niobium (100) face. Both krypton and neon were also shown to be face-centered cubic on the basis of their LEED intensities and, in fact, sufficiently large krypton and neon crystallites could occasionally be grown to show definite threefold symmetry superimposed on the residual pseudo-12-fold symmetry.

Xenon (Fig. 5), however, did not condense with a (111) face parallel to a Nb (100) substrate under the conditions studied (~6–60 °K and rates of

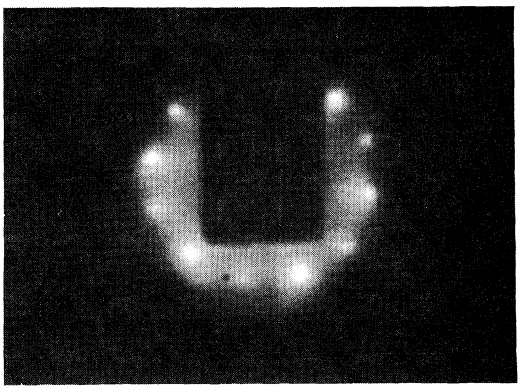

FIG. 3. LEED pattern from the (111) face of argon adsorbed on Nb(100). Four distinct domains are present.

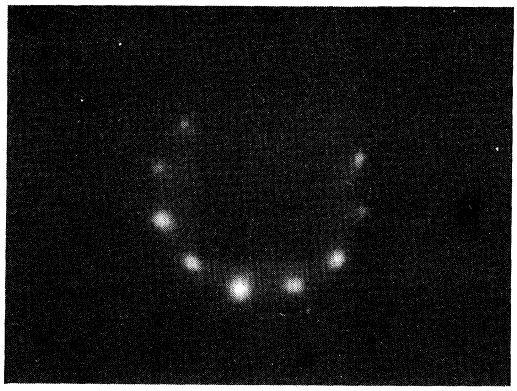

FIG. 4. LEED pattern from the (111) face of krypton adsorbed on Nb(100). Four distinct domains are present.

deposition between 0.05 and 2 Langmuir) (1 Langmuir is exposure to gas at 10^{-6} Torr for 1 sec). Several different variations were observed that all appeared to be related to the formation of a xenon (100) face slightly out of register with the niobium substrate. In the presence of minute quantities of niobium oxide on the substrate surface, xenon produced large diffuse diffraction features in the $c(2\times2)$ position at temperatures somewhat below liquid-nitrogen temperature. At 7 °K, these diffuse features had segregated into a quartet of four diffraction spots centered approximately around the $c(2\times2)$ position. When xenon was crystallized onto a niobium substrate at 7 °K in the absence of any niobium oxide, what appeared to be a poorly defined (7×7)-45° structure with strong features in the $(\frac{2}{7}\frac{5}{7})$, $(\frac{3}{7}\frac{4}{7})$, $(\frac{4}{7}\frac{3}{7})$, and $(\frac{5}{7}\frac{2}{7})$ was observed. The $(\frac{3}{7}\frac{4}{7})$ and $(\frac{4}{7}\frac{3}{7})$ spots appeared to be the same as two of the member of the previously described quartet. When this structure was annealed, pure Xe (111) crystallites could be grown that were at least as large as the diameter of the LEED beam, i.e., 1 mm or larger.

At 100 °K, the two-dimensional unit mesh in the xenon (100) face is characterized by a lattice parameter of 4.36 Å which is about 6% smaller than the Nb (100)-$c(2\times2)$ distance of 4.66 Å. Thus, it is probable that the xenon attempts to grow with its (100) face parallel to the niobium (100) face with xenon atoms occupying every other position in the substrate unit mesh. At the higher temperatures, the xenon lattice parameter will be closer to that of the niobium and this, possibly coupled with the relatively high thermal motion of the xenon atoms at these temperatures, may be adequate to produce the observed diffuse $c(2\times2)$ patterns. At lower temperatures, the mismatch will become more severe and misalignment may occur. Thus, the quadrupling of these features at the low temperatures may result from the option of our different crystallographically equivalent directions in the substrate relative to which misalignment may occur. It is possible that the presence of a small amount of niobium oxide (which has fourfold symmetry and a lattice parameter slightly smaller than niobium[9]) may provide nucleation sites for the growth of relatively large ($>\sim50$ Å) xenon (100) crystals, while its absence forces the growth of relatively small ($<\sim50$ Å) xenon (100) crystallites, which give rise to the more complicated diffraction patterns observed for xenon on the very clean niobium substrates. However, the information available for this more complicated structure is, because of the poor quality of the diffraction patterns, too limited to allow for a more detailed analysis.

The majority of the Auger and energy-loss spectra were done on this structure, while most of the LEED intensity data reported below were performed on the annealed Xe(111) structure.

IV. INTENSITY DATA

All of the intensity data reported in this paper were performed on the first-order diffraction beams from the various crystalline faces near normal in-

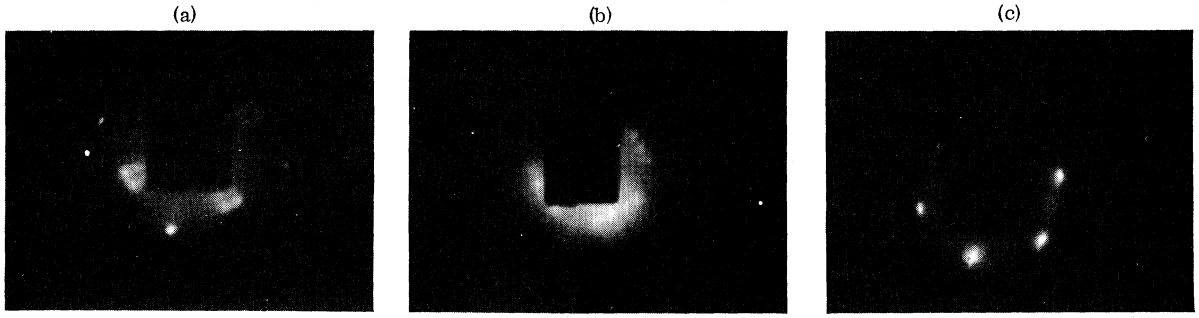

FIG. 5. LEED patterns from xenon adsorbed on the (100) face of niobium. (a) Diffraction pattern from (100) face of Xe adsorbed near liquid-helium temperatures in the presence of a trace of an oxide on the niobium surface. Note quadrupling of diffraction features. These are not resolved at higher temperatures. (b) Diffraction pattern from Xe adsorbed near liquid-helium temperatures on a clean Nb(100) surface. (c) Diffraction pattern from the (111) face of Xe obtained by annealing structure shown in (b).

cidence. Because of the rapid desorption rates of neon and argon, it was impossible to obtain high-quality intensity vs energy plots. It was, however, possible to make visual estimates of the energy positions of the intensity maxima. However, krypton data of fair quality and xenon data of excellent quality for the (111) face were obtained.

The (111) face of face-centered-cubic crystals has threefold symmetry. Thus, there are two types of first-order diffraction beams. In the kinematic approximation, these two types of beams will have intensity maxima at different electron energies. However, at lower energies, these two types of maxima will fall relatively close together and form doublets. When the actual crystalline domains were sufficiently small, the resulting diffraction patterns were composed of beams that were superpositions of both types of domains. As we did not consistently grow large single crystals of neon, argon, or krypton, the resulting intensity data reflect this superposition. The visual estimates of intensity maxima fall within the doublet region, while the photometrically measured curves for krypton show this doubling in detail. The data for xenon were measured from relatively large single crystals and resulted in relatively pure spectra. As was found by Ignatjevs, Pendry, and Rhodin for the (00) beam from Xe(111), the data are relatively kinematic, particularly in the higher voltage regions.[9] However, at lower voltages, there is definite dynamical behavior (e.g., 60-eV region on xenon). This relatively kinematic behavior may be, in part, a manifestation of the large Debye-Waller factors and strong inelastic processes that will be discussed below. An alternative explanation evokes a certain amount of strain or disorder on the surface of the crystal.

The intensity vs energy curves for krypton and xenon are given in Figs. 6 and 7, and the measured and estimated intensity maxima positions for all of the gases are given in Table I along with values calculated from a free-electron or kinematic model.

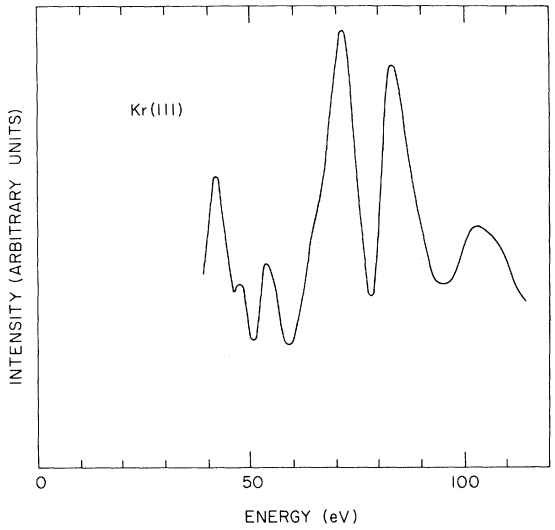

FIG. 6. Intensity of the first-order diffraction beam from the (111) face of krypton as a function of energy near normal incidence. Several domains were present simultaneously so that the resulting diffraction features were superpositions of first-order diffraction beams of both types.

V. CHARACTERISTIC-ENERGY-LOSS SPECTRA

The kinematic nature of the intensity vs energy plots for the diffracted beams and the large desorption rates of the lighter inert-gas crystals indicated the possible existence of unusual inelastic interactions between the incident electrons and the crystalline films. To investigate these interactions, we made a fairly detailed study of the characteristic-energy-loss spectra, which is discussed in the following paper.[1] Those features that are pertinent to this paper are as follows. (a) We observed large losses for all of the inert-gas crystals in the general vicinity of the niobium plasmon-loss region (e.g., ~10–20 eV). (b) These losses were much larger than generally observed in metallic systems. (c) Unlike plasmon losses, those for the inert-gas crystals corresponded to the excitation of single electrons to higher lying excited states rather than the excitation of collective modes.

In general, in this energy region we were observing the excitation of an electron from the outermost filled p level (e.g., $2p$ for neon) to a higher lying state. For the lighter gases, these excitations are fairly localized and the resulting spectra are similar to those for free atoms in the gaseous state. For the heavier inert gases there is a considerable overlap in the excited state and the excitations are more delocalized so that the resulting spectra more closely resemble those for Wannier excitons. In addition to losses of this type, we have also observed losses at higher energies that correspond to the excitation from inner electronic shells (e.g., $5s$ and $4d$ for Xe). In Fig. 8 we show a typical characteristic-loss spectra for Ne.

VI. DESORPTION

One of the more interesting features of this study was the rapid desorption rates of neon, argon, and, to a lesser extent, krypton when exposed to the electron beam under conditions where it was possible to maintain these crystals for long periods of time in the absence of the electron beam. With neon, for example, this desorption allowed several minutes working time near 30-eV primary energy but this time was reduced by about two orders of magnitude near 100 eV. In Fig. 9 we show the desorption of neon with several pri-

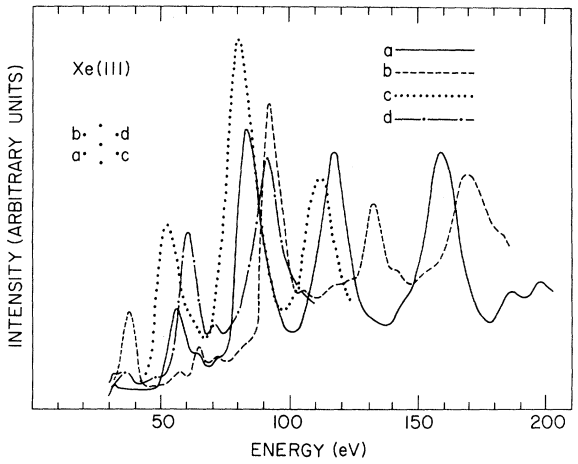

FIG. 7. Intensity of several first-order diffraction beams from the (111) face of xenon as a function of energy. Essentially one single crystal of xenon was present, so there is little superposition of beams from domains of different orientations. The data were obtained near, but not precisely at, normal incidence so that diffraction beams of the same type, e.g., *a* and *c* or *b* and *d*, do not provide coincidental intensity vs energy plots.

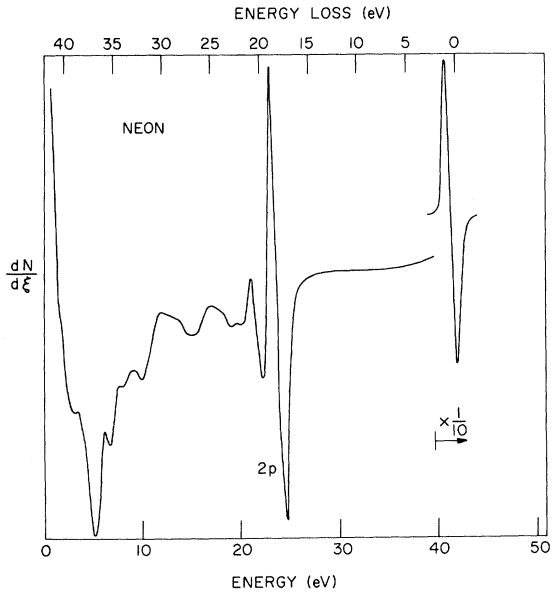

FIG. 8. Characteristic-energy-loss spectra from the (111) face of neon obtained with 42-eV primary electrons. Qualitative desorption rates were obtained by monitoring the height of the large loss peak at about 17 eV below the primary peak.

mary electron energies as measured by the height of the 17-eV-electron-energy-loss peak in the loss spectrum. The neon crystals for the 40-, 50-, and 60-eV measurements were about 20 monolayers thick while that for the 30-eV measurement was somewhat thinner. Note the rapid increase in desorption rate with primary energy. The initial transient period of an apparent lower rate is probably due to saturation of the energy-loss spectrum owing to the limited penetration of the electrons.

These data are meant to be qualitative rather than quantitative since certain experimental parameters (such as the current density) were not closely controlled. In fact, the data varied markedly from day to day. Current densities were in the vicinity of 5 $\mu A/mm^2$ at 50 eV and considerably less at the lower voltages.

TABLE I. Energy (eV) of intensity maxima in the first-order diffraction beams from the (111) face of Ne, Ar, Kr, and Xe.

Ne		Ar		Kr		Xe	
Calc.	Expt.	Calc.	Expt.	Calc.	Expt.	Calc.	Expt.
35	36–40	24		24	26	19	21
52	58–62	36	38	36	31	29	25
69		48	45	48	45	38	36
87		60	65	60	55	47	44
104	103–110	72		72	74	57	58
121		84	80	84	85	66	67
138		96		96		76	
			107		108		86
			122				

In Fig. 10 we show the desorption of neon with approximately 30-eV primary electrons as measured by the height of the electron-energy-loss peak and as measured by the intensity of one of the first-order LEED beams. These two techniques are sensitive to two different quantities. Outside of the saturation region, the height of the electron energy-loss peak is roughly proportional to the number of neon atoms on the substrate surface, while the intensity of the LEED beam is proportional to the square of the number of atoms present in an ordered fashion. Note the initial rise in the intensity curve. This most probably corresponds to a slight annealing of a mildly disordered crystal with the electron energy available from the incident electrons.

In Fig. 11 the desorption of argon is shown for several primary energies. Though precise comparisons are difficult because of the qualitative nature of the data, it would appear that the desorption rates for argon are considerably larger than those for neon at low energies. This is consistent with general observation and with the previously published data on the decrease in the intensity of the LEED beams from argon.

Krypton was considerably more resistant to erosion by the incident electrons than either argon or neon. The proximity of the dominant krypton characteristic-energy-loss peaks to the niobium plasmon-energy-loss peaks made it rather diffi-

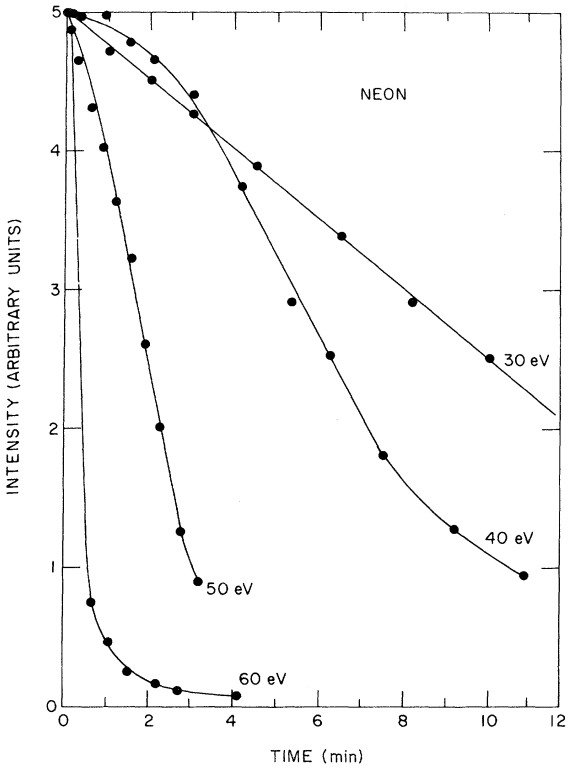

FIG. 9. The desorption of neon by electrons with several different energies as measured by monitoring the decrease in the height of the dominant peak in the neon characteristic-energy-loss spectrum as a function of time.

cult to study the desorption by this technique. In Fig. 12 data for the desorption of krypton as measured by both LEED and the energy-loss spectrum are shown. The apparent larger desorption rate measured at 70 eV by LEED relative to that at 80 eV measured by the energy-loss spectrum is most likely an artifact of the N^2 dependence of the LEED intensity vs the N dependence of the intensity of the energy-loss measurements.

Xenon was essentially completely resistant to desorption by the incident electrons over the time scale of the experiment (several hours). No deterioration in the quality of the LEED patterns or the loss spectrum was noted.

In this first study we were not able to control some of the important parameters which may be relevant to the rate of desorption, e.g., the temperature and, particularly, the electron current density. Thus the data we have just described cannot be compared with a quantitative theory, but it is evident that the rate of desorption decreases in the sequence Ar, Kr, and Xe, with Ne possibly occupying an anomalous position after Ar. There are three possible ways in which the energy of the incident electrons may cause the desorption: as a

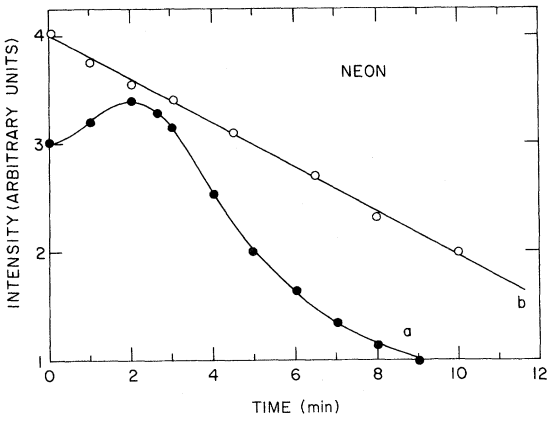

FIG. 10. The desorption of neon with approximately 30-eV electrons as measured by two different techniques. In curve (a) the intensity of the first-order LEED beam at 33 eV is monitored as a function of time. In curve (b) the intensity of the dominant characteristic-energy-loss peak for 30-eV primary electrons is measured as a function of time.

purely thermal effect, or by resulting in the ejection of an atom after either an elastic or inelastic scattering event. The latent heats of the rare gases are listed in Table II and, as can be seen, are very small so that little energy is required to eject an atom from the solid compared to a metal.

First, we must consider possible heating of the sample by the electron beam, although, of course, not all the energy brought in by the electron beam is converted into heat in the sample. A quick calculation shows that at the current densities used the total power input of the electron beam is about 5×10^{-4} W/mm^2. This is comparable to the energy of thermal radiation from room termperature in-

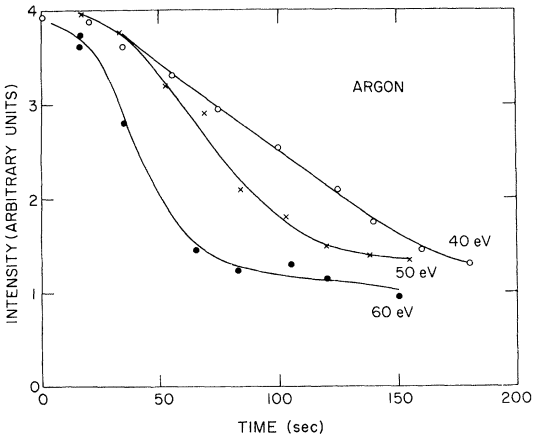

FIG. 11. The desorption of argon by electrons with several different energies as measured by monitoring the decrease in the height of the dominant peak in the argon characteristic-energy-loss spectrum.

cident on the crystal. In the absence of the electron beam, the rare-gas crystals are not noticeably desorbed after several hours, so this level of energy input, by itself, is not sufficient to vaporize the crystal. The difference in the two situations is that the room-temperature photons have a probable energy of about 0.1 eV, which is several orders of magnitude lower than the energy of the electrons and also much less than the energy required to create an electronic excitation in the solid.

The second possibility is that the energy acquired by an atom when an electron is elastically scattered is sufficient to eject the atom from the solid. Because of conservation of momentum, the maximum energy that can be transferred is $4Em/M$, where E is the energy of the electron and M is the effective mass of the atom, which may be larger than the free mass for an atom bound to a solid. This mechanism is regarded as responsible for sputtering but, in order to cause sputtering of metals, it is necessary to use gas atoms as projectiles and it is unlikely that electrons have ever caused sputtering of metals.[10] However, the binding energy of the rare gases is an order of magnitude lower than that of metals, so it is conceivable

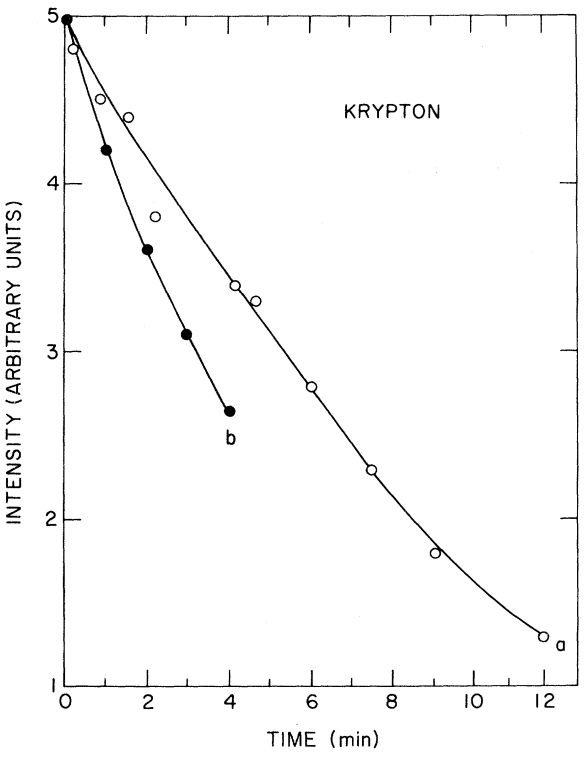

FIG. 12. The desorption of krypton as measured (a) by monitoring the height of a characteristic-energy-loss peak with 80-eV primary electrons and (b) by monitoring the intensity of a LEED first-order diffraction beam at 70 eV.

TABLE II. Latent heats of the rare gases.

	Mass (amu)	Latent heat (eV)	Nearest-neighbor distance (Å)
Ne	20	0.02	3.0
Ar	40	0.08	3.5
Kr	84	0.11	3.8
Xe	131	0.15	4.1

that electrons could sputter the rare gases. In sputtering, the yields correlate with sublimation energy, as might be expected. By this mechanism, Ne would probably be the most easily detached because it has the smallest mass and least binding energy and the other rare gases would be increasingly harder to detach in order of increasing atomic number. For a 100-eV electron, the maximum energy acquired by an Ar atom would be about 10^{-3} eV, which is an order of magnitude less than the binding energy of 0.04 eV. Although the cross section for elastic scattering of electrons is high in the energy range used, little energy is transferred so this process is unlikely to be the principal cause of the rapid desorption.

As mentioned earlier, the electron beam loses energy by inelastic collisions and some of this energy could cause desorption. The inelastic scattering results in the excitation of an electron into a higher electronic state or even the expulsion of an electron. Before this excitation can decay it is possible that the excited atom or ion may leave the crystal. This process has, in fact, been observed in many cases of adsorbed layers of atoms on metal surfaces, principally, CO, H, O, and N, and is known as electron-impact desorption[10] (EID) and is the analog for a solid of Franck–Condon dissociation of molecules. The latent heats of the rare gases are comparable with the heats of physisorption and chemisorption so a similar process may be obtain here.

The main features of EID for adsorbed atoms have been discussed by Redhead[11] and by Menzel and Gomer[12] and can be explained briefly as follows. Using the usual adiabatic approximation to separate the electronic and nuclear motion, one finds that the nuclear configuration does not change appreciably during the electronic transition to a higher state. This may result in the electronically excited atom being in a position of high vibrational potential energy, and thus being able to escape the solid during its relaxation if the kinetic energy acquired is greater than the binding energy. A similar argument applies if the loss mechanism has resulted in the ejection of an electron forming an ion rather than an excited atom. For an atom to be ejected, the lifetime of the excited electronic

state must be longer than the relaxation time of the atom, which is about 10^{-14} sec. It was observed for cases other than the inert gases that the desorption cross sections usually are much smaller than the inelastic cross section. This was attributed to the short lifetime of the excited electronic state, which is thus usually the limiting factor. This explains why ejection is so rare and why EID depends not only on the adsorbed atom, but also on the state in which it is adsorbed.[11,12] In a particular case the probability of desorption is determined by both the probability of excitation, i.e., the appropriate cross section, and by the lifetime of the excited state.

In general it must be remembered that we are dealing with excited states of a solid, not an isolated atom, and thus the excitations are really excitons, either the Frenkel tightly bound type or the Wannier loosely bound type. In fact, the large loss peak near 17 eV shown in Fig. 8 for neon corresponds to a Frenkel exciton. In this language, removal of an atom will depend on the lifetime of the exciton and also the extent to which it can be associated with a particular atom. It is probable that the Frenkel excitons are the principle agents in desorption. This point may be relevant to the case of Xe, whose desorption rate is essentially negligible and where the excitons are expected to be more Wannier-like, and therefore more delocalized, because of the greater polarizability. Since the inelastic scattering cross sections are known for the gases, and it is probable that the cross sections in the solids are similar, one can say that the cross sections for Ar, Kr, and Xe are similar and Ne is less by about a factor of 10. Hence the negligible desorption of Xe cannot be explained on this basis. The higher masses and binding energies of the heavier gases will certainly play a role, but the nonlocalized character of the excitation might also be an important factor. This should occur because the excited electron is now separated from the atom with the hole and the desorption process must involve an ion, and second, there is possibly less vibrational energy given to an individual atom than in the Frenkel-exciton case.

We also emphasize that we are concerned with crystals that are only about 20 layers thick and it is possible that the surface plays an important role in the desorption process.

ACKNOWLEDGMENTS

We would like to acknowledge discussions with many colleagues and, in particular, we are indebted to Professor D. L. Dexter and Professor John Hudson. In addition, O. F. Kammerer and T. F. Arns provided invaluable technical assistance.

---

*Work performed under the auspices of the U.S. Atomic Energy Commission.

[1]H. H. Farrell and M. Strongin, following paper, Phys. Rev. B 6, 4711 (1972).

[2]J. M. Dickey, H. H. Farrell, and M. Strongin, Surface Sci. 23, 448 (1970).

[3]M. Strongin, J. M. Dickey, H. H. Farrell, T. F. Arns, and G. Hrabak, Rev. Sci. Instr. 42, 311 (1971).

[4]The difference in free energy between the hcp and the fcc modifications is rather small (Ref. 5). In fact, the hcp modifications of Ar and Ne have been observed in metastable and/or impurity stabilized situations (Refs. 5–7).

[5]J. A. Venables and C. A. English, Thin Solid Films 7, 369 (1971).

[6]L. Meyer, C. S. Barret, and P. Haasen, J. Chem. Phys. 40, 2744 (1964).

[7]O. Bostanjoglo and R. Kleinschmidt, J. Chem. Phys. 46, 2004 (1967).

[8]J. M. Dickey, H. H. Farrell, O. F. Kammerer, and M. Strongin, Phys. Letters 32A, 483 (1970).

[9]A. Ignatjevs, J. B. Pendry, and T. N. Rhodin, Phys. Rev. Letters 26, 189 (1971).

[10]P. A. Redhead, J. P. Hobson, and E. V. Koraelson, in *The Physical Basis of Ultra High Vacuum* (Chapman Hall, London, 1968).

[11]P. A. Redhead, Can. J. Phys. 42, 886 (1964).

[12]D. Menzel and R. Gomer, J. Chem. Phys. 41, 3311 (1964).

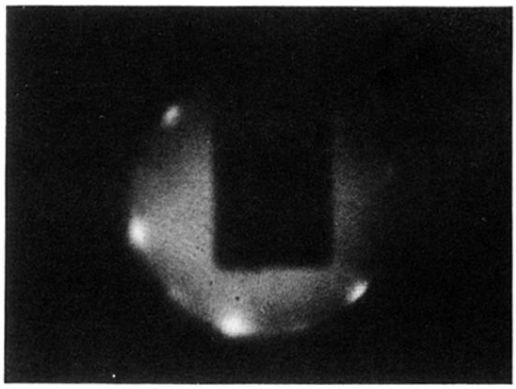

FIG. 2. LEED pattern from the (111) face of neon adsorbed on Nb(100). Dark rectangle in foreground is a cryogenic shield surrounding the sample. Note trace of pseudo-12-fold symmetry.

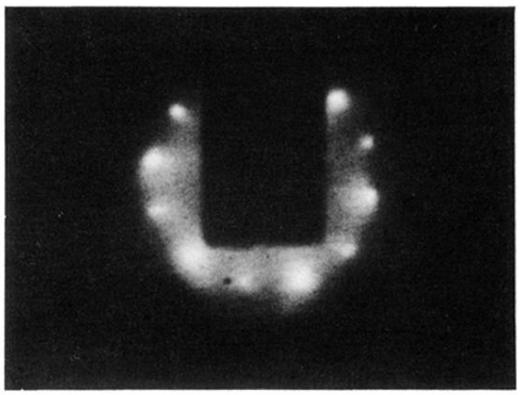

FIG. 3. LEED pattern from the (111) face of argon adsorbed on Nb(100). Four distinct domains are present.

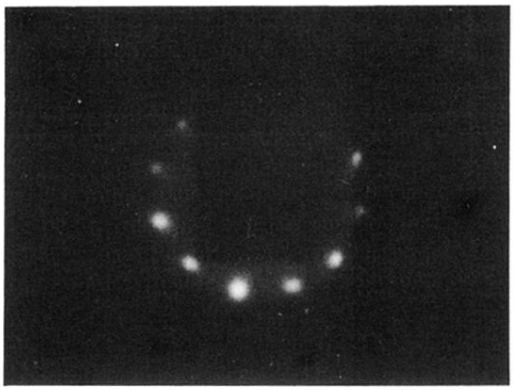

FIG. 4. LEED pattern from the (111) face of krypton adsorbed on Nb(100). Four distinct domains are present.

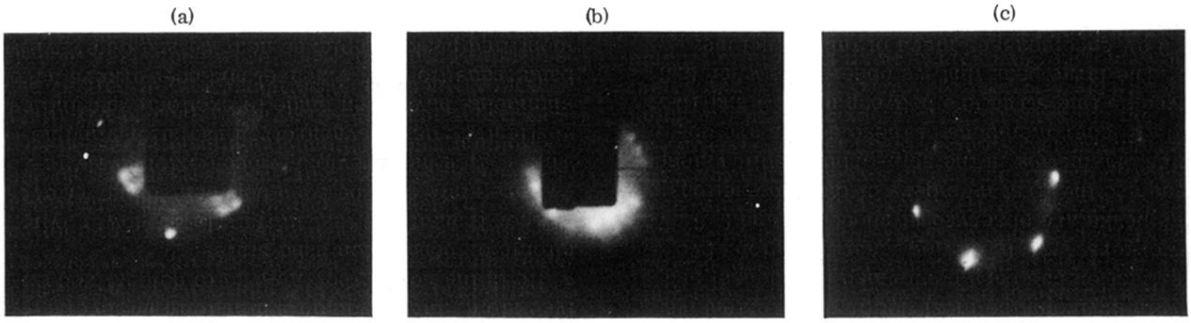

FIG. 5. LEED patterns from xenon adsorbed on the (100) face of niobium. (a) Diffraction pattern from (100) face of Xe adsorbed near liquid-helium temperatures in the presence of a trace of an oxide on the niobium surface. Note quadrupling of diffraction features. These are not resolved at higher temperatures. (b) Diffraction pattern from Xe adsorbed near liquid-helium temperatures on a clean Nb(100) surface. (c) Diffraction pattern from the (111) face of Xe obtained by annealing structure shown in (b).